Article

Small-molecule inhibition of the *C. difficile* FAS-II enzyme, FabK, results in selective activity

Jesse A. Jones, Allan M. Prior, Ravi K. R. Marreddy, Rebecca D. Wahrmund, Julian G. Hurdle, Dianqing Sun, and Kirk E. Hevener

ACS Chem. Biol., **Just Accepted Manuscript** • DOI: 10.1021/acschembio.9b00293 • Publication Date (Web): 11 Jun 2019

Small-molecule inhibition of the *C. difficile* FAS-II enzyme, FabK, results in selective activity

Jesse A. Jones,[a]* Allan M. Prior,[b]* Ravi K.R. Marreddy,[c] Rebecca D. Wahrmund,[a] Julian G. Hurdle,[c] Dianqing Sun,[b#] Kirk E. Hevener,[a#]

[a]Department of Pharmaceutical Sciences, College of Pharmacy, University of Tennessee Health Science Center, Memphis, Tennessee, 38163, United States

[b]Department of Pharmaceutical Sciences, The Daniel K. Inouye College of Pharmacy, University of Hawaii at Hilo, Hawaii, 96720, United States

[c]Center for Infectious and Inflammatory Diseases, Institute of Biosciences and Technology, Texas A&M Health Science Center, Houston, Texas, 77030, United States

Running Head: Selective Inhibition of *C. difficile* FabK

#Address correspondence to Kirk E. Hevener, khevener@uthsc.edu and Dianqing Sun, dianqing@hawaii.edu.

*J.A.J. and A.M.P. contributed equally to this work.

Abstract

Clostridioides difficile infection (CDI) is a leading cause of significant morbidity, mortality, and healthcare-related costs in the United States. After standard therapy, recurrence rates remain high and multiple recurrences are not uncommon. Causes include treatments employing broad-spectrum agents that disrupt the normal host microbiota, as well as treatment-resistant spore formation by *C. difficile*. Thus, novel druggable anti-*C. difficile* targets that promote narrow-spectrum eradication and inhibition of sporulation are desired. As a critical rate-limiting step within the FAS-II bacterial fatty acid synthesis pathway, which supplies precursory component phospholipids found in bacterial cytoplasmic and spore-mediated membranes, enoyl-acyl carrier protein (ACP) reductase II (FabK) represents such a target. FabK is essential in *C. difficile* (*Cd*FabK) and is structurally and mechanistically distinct from other isozymes found in gut microbiota species, making *Cd*FabK an attractive narrow-spectrum target. We report here the kinetic evaluation of *Cd*FabK, the biochemical activity of a series of phenylimidazole analogues, and microbiological data suggesting these compounds' selective antibacterial activity against *C. difficile* versus several other prominent gut organisms. The compounds display promising selective, low micromolar *Cd*FabK inhibitory activity without significantly affecting the growth of other gut organisms, and the series prototype (**1b**) is shown to be competitive for the *Cd*FabK cofactor and uncompetitive for the substrate. A series analogue (**1g**) shows maintained inhibitory activity while also possessing increased solubility. These findings represent the basis for future drug discovery efforts by characterizing the *Cd*FabK enzyme while demonstrating its druggability and potential role as a narrow-spectrum anti-difficile target.

Keywords: *Clostridioides difficile*, enoyl-ACP reductase II, FabK, phenylimidazole, enzyme inhibitor, antibacterial, narrow-spectrum

Clostridioides difficile (formerly *Clostridium difficile*) is a Gram-positive, spore-forming, anaerobic pathogen that is the leading cause of health care-associated diarrhea and gastroenteritis-associated deaths in the U.S.[1, 2] Clinical consequences of *C. difficile* infection (CDI) range from asymptomatic or mild diarrhea to recalcitrant diarrhea and fatal pseudomembranous colitis.[3] CDI is caused by the eradication of key gut flora, such as *Bifidobacterium* sp. and *Bacteroides* sp., which normally suppress *C. difficile* overgrowth.[4] This typically occurs via the use of broad-spectrum antibiotics (e.g., clindamycin, fluoroquinolones, and beta-lactams).[4-6] The first-line CDI treatment, vancomycin, exhibits activity against beneficial gut flora and results in their eradication, contributing to high rates of recurrence.[7, 8] Further contributing to relapse is the pathogen's ability to produce treatment-resistant spores that survive in the intestinal tract.[9, 10] The emergence of epidemic strains, namely BI/NAP1/027 (North American pulsed-field gel electrophoresis type 1, ribotype 027), correlated with an increase in incidence and severity of CDI.[7] While the alternative first-line drug fidaxomicin is narrow-spectrum and reduces recurrence, it has failed to show evidence of doing so in NAP1-mediated infections.[11, 12] Fecal microbiota transplantation (FMT) shows promise, but long-term safety data is still lacking, including non-infectious microbiota-related metabolic diseases like obesity.[13, 14] While new agents are currently in clinical trials, recent failures highlight the pressing need for novel anti-CDI agents to maintain the discovery pipeline.[6, 15] These issues emphasize that *C. difficile* remains a high-priority candidate for the development of novel narrow-spectrum antibacterial agents.

During cyclic fatty acid elongation within the bacterial type II fatty-acid synthesis (FAS II) pathway, enoyl-acyl carrier protein (ACP) reductase enzymes catalyze the critical, rate-limiting terminal reduction step. The FAS-II system provides fatty acid precursory components vital to bacterial organisms for various biological processes like membrane phospholipid production and sporulation.[16] Strong scientific precedent substantiates these enzymes as antimicrobial drug targets, exemplified by isoniazid, a marketed inhibitor of tubercular InhA (enoyl-ACP reductase); triclosan, a well-known antibacterial FabI inhibitor; and the anti-staphylococcal FabI inhibitor afabicin (Debio-1450) currently in clinical trials.[17-20] While the existence of four distinct enoyl reductase isozymes (FabI, FabK, FabL, and FabV) in bacteria precludes the development of broad-

spectrum antibacterials targeting them, it affords an ideal opportunity for the rational design of narrow-spectrum agents.[21-23] Bioinformatics analyses of sequenced *C. difficile* genomes indicate it expresses the FabK isozyme as its sole enoyl-ACP reductase.[24, 25] FabK, a member of the triosephosphate isomerase (TIM) barrel family of proteins, is a less abundant isozyme among the four enoyl-ACP reductases, and lacks sequence similarity to FabI, FabL, and FabV, which are members of the short-chain alcohol dehydrogenase/reductase (SDR) superfamily (**Figure 1**).[22, 26] Like the other isozymes, FabK requires either NADH or NADPH as a cofactor for activity, but unlike its SDR counterparts, FabK is a flavoenzyme that utilizes flavin mononucleotide (FMN) as an active site prosthetic group. FabK is also unique in that it uses a bi-bi double displacement (Ping-Pong) enzymatic mechanism for reducing its enoyl substrate.[22, 26-33] The SDR enzymes, however, possess a classical Rossman fold for binding their NAD(P)H cofactor and rely on an ordered sequential enzyme mechanism for reducing their enoyl substrates.[34, 35] While there has been recent debate about the essentiality of the FAS-II pathway in Gram-positive bacteria,[36-38] several groups have shown that possession of the FapR regulatory system over FabT, as seen in *S. aureus,* prevents full bypass of FAS-II inhibition by exogenous fatty acid uptake.[39, 40] Indeed, we recently showed that *C. difficile*, which also possesses FapR, behaves in a similar manner as exogenous fatty acids were unable to rescue the pathogen from FAS-II inhibition.[25] *C. difficile* also has unique branched fatty acid requirements, further limiting the likelihood of escape from FAS-II inhibition.[41, 42] Our recent work also demonstrated the ability of FAS-II inhibition to decrease spore formation by nearly 90%, which in principle could reduce potential for spore survival, associated endogenous recurrence, and spore dissemination.[25]

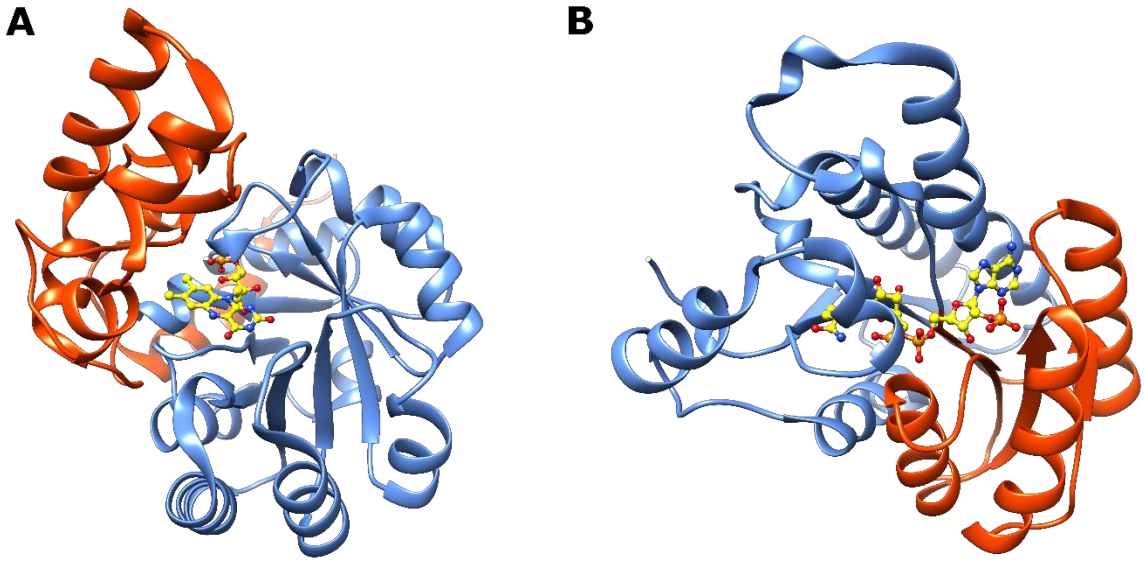

Figure 1. Comparison of FabK and FabI Structures with Bound Cofactors. A. *P. gingivalis* FabK structure (PDB 4IQL) shows the C-terminal domain in orange and the conserved TIM barrel domain in blue. The FMN prosthetic group is shown as ball & stick structure with yellow carbons. **B.** The *S. aureus* FabI structure represents the SDR protein family structure shared by FabI, FabL, and FabV. The conserved Rossman fold is shown as orange ribbons and the NADPH cofactor is shown as ball & stick structure with yellow carbons.[43]

CDI pharmacotherapy has shown that maximizing therapeutic success includes preventing collateral damage to the GI microbiome. Important gut species such as Gram-negative *Bacteroides* sp.[44] express FabI with or without FabK, while *Bifidobacterium* sp. lack FabK entirely.[25] Importantly, published FabK inhibitors are inactive against FabI and FabI-bearing strains.[29, 32] Similarly, FabK has demonstrated resistance to FabI inhibitors like triclosan, which are consequently inactive against strains carrying FabK.[22, 27, 45, 46] Lastly, the ability of bacterial strains carrying two enoyl reductases to survive the deletion of one isozyme suggests that both enzymes would need to be dually inactivated to inhibit the growth of such organisms.[21] This data justifies the investigation of FabK as a narrow-spectrum target for selective anti-difficile therapy.

FabK from *S. pneumoniae* (*Sp*FabK) was shown by Takahata et al. to be specifically inhibited by a compound (AG-205) they found during a high throughput screening campaign, which led to the development of the more potent phenylimidazole-derived class of inhibitors via iterative medicinal chemistry modifications (e.g., replacing the amide linker with urea functionality, exploring various substitutions at the solvent exposed head region, un-fusing the benzimidazole ring systems, and evaluating various substitutions at the tail region).[29-33] Despite substantial gains in potency, further development was ceased, possibly due to the unfortunate fact that *Streptococci* are able to bypass FAS-II inhibition as they carry the FabT regulatory system.[36] Because *C. difficile* harbors the FapR regulatory system, it presents an opportunity to renew the development of phenylimidazole FabK inhibitors.[25] In an effort to characterize the enzyme target, we therefore performed essential kinetic evaluations of *Cd*FabK, including substrate and cofactor K_m determinations, inhibition modality, and substrate inhibition effects. We also report that phenylimidazoles display potent on-target biochemical activity against *Cd*FabK (**Table 1**) and are amenable to modifications that improve physiochemical properties (**Scheme 1**; Materials and Methods) while maintaining biochemical and anti-*C. difficile* activity, and demonstrate a promising, narrow-spectrum antibacterial profile against *C. difficile* over key members of the gut flora (**Table 2**).

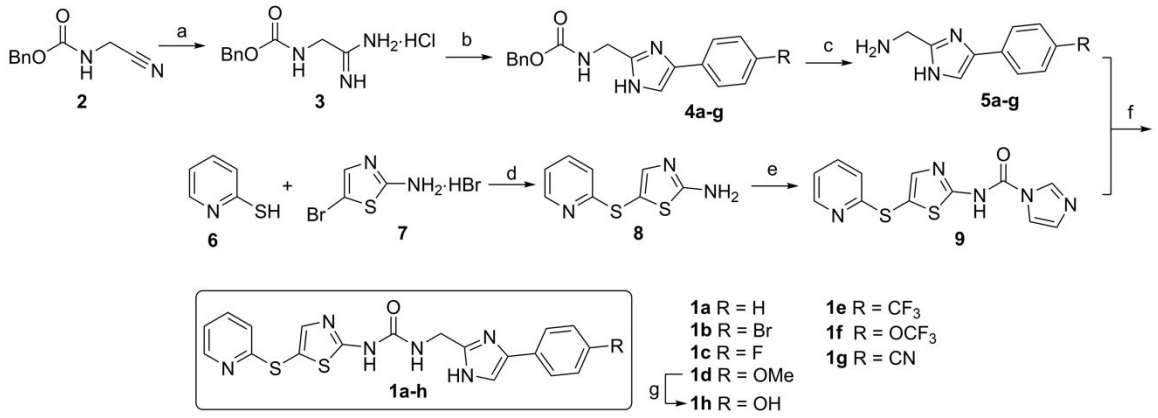

Scheme 1. Synthesis of phenylimidazole derivatives 1a-h. [a]Reagents and conditions: (a) i. NaOMe, MeOH, 25 ºC, 8 h; ii. NH_4Cl, 25 ºC, 3 days, 91%; (b) substituted 2-bromoacetophenone, K_2CO_3, THF/H_2O (10:1), reflux, 18 h; (c) HCl, H_2O, reflux, 3 h, 27-69% (over 2 steps); (d) K_2CO_3, DMF, 80 ºC, 1.5 h, 67%; (e) CDI (2 equiv.), DCM, 25 ºC, 18 h, 74%; (f) Et_3N, $CHCl_3$, 25 ºC, 2 h, 30%-89%; (g) BBr_3, DCM, 0-25 ºC, 45 min, 92%.

Table 1. Inhibitory activity of Enoyl-ACP isozymes by phenylimidazole analogues.

Compound	***Cd*FabK IC_{50} [95% CI]; % Inhibition at 10 μM**	***Sp*FabK IC_{50} [95% CI]**
Triclosan	>100 μM	>100 μM
1a	>10 μM; 38.51%	0.730 μM [0.434, 1.456]
1b	3.31 μM; 95% CI [2.68, 4.19]	0.067 μM [0.054, 0.084]
1c	>10 μM; 49.86%	0.242 μM [0.214, 0.274]
1d	>10 μM; 44.80%	0.198 μM [0.178, 0.222]
1e	2.86 μM [2.02, 4.35]	0.078 μM [0.066, 0.093]
1f	4.63 μM [3.12, 8.02]	0.163 μM [0.124, 0.214]
1g	7.35 μM [5.35, 11.65]	0.085 μM [0.072, 0.101]
1h	>10 μM; 35.58%	0.538 μM [0.433, 0.675]
AG-205	4.15 μM [3.324, 5.597]	5.32 μM [4.378, 6.809]

CI, Confidence Interval

Table 2. MIC values in the presence and absence of efflux inhibitor verapamil suggesting inhibitors are specific for FabK

Organism	Enoyl-ACP reductase	MIC (μM) (-) Verapamil					MIC (μM) (+) Verapamil				
		1b	**1e**	**1f**	**1g**	**VAN**	**1b**	**1e**	**1f**	**1g**	**VAN**
C. difficile R20291	FabK	4	8	8	8	1.6	4	2	2	2	0.8
S. pyogenes ATCC19615†	FabK	0.125	<0.0625	<0.0625	0.125	0.2	0.125	<0.0625	<0.0625	0.125	0.4
C. perfringens HM310	FabI	>128	>128	>128	>128	6.4	>128	>128	>128	>128	6.4
B. ovatus ATCC8485	FabI & FabK	>128	>128	>128	>128	6.4	>128	>128	>128	>128	6.4
B. fragilis ATCC25285	FabI	>128	>128	>128	>128	3.2	>128	>128	>128	>128	3.2
B. breve ATCC 11863	*	>128	>128	>128	>128	3.2	>128	>128	>128	>128	3.2

*Yeast like fatty acid synthase

† *Streptococcus* species harbor the FabT regulatory system, allowing for bypass of FASII inhibition in the presence of exogenous fatty acids.[25]

Results

The *Cd*FabK enzyme possesses intrinsic NADH oxidative activity and double substrate inhibition.

The *Cd*FabK enzyme displayed NADH oxidative activity in the absence of enoyl substrate (**Figure 2**). Apparent K_m (K_m^{app}) values were determined via 1.5-fold serial dilutions of the NADH cofactor while holding the enoyl substrate, crotonyl coenzyme A (Cro-CoA), constant at 150 μM; likewise, 1.5-fold serial dilutions of Cro-CoA were tested while holding the NADH cofactor constant at 150 μM; and an alternative enoyl substrate, octenoyl coenzyme A (Oct-CoA), was tested similarly via 1.5-fold dilutions while holding NADH constant at 150 μM. Initially, K_m^{app} values were determined via standard Michaelis-Menten non-linear regression fits. However, upon further analysis, the data for cofactor and substrates all fit a substrate inhibition model (R^2 = 0.9854; 0.7607; and 0.8479, respectively) better than the poorly fit standard Michaelis-Menten models. As such, respective K_m^{app} values for NADH, Cro-CoA, and octenoyl coenzyme A were determined to be 138.1 μM, 327.0 μM, and 420.8 μM, as opposed to 23.0 μM, 176.0 μM, and 65.5 μM observed with the standard Michaelis-Menten model, respectively.

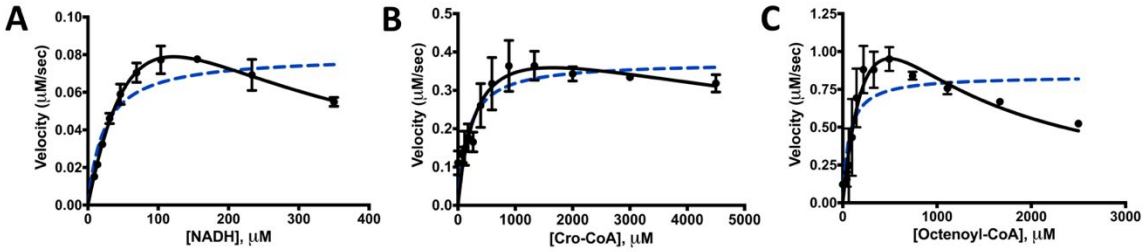

Figure 2. Enzyme Kinetics of *Cd*FabK vs. Velocity. (A) Non-linear regression curve fit of velocity of *Cd*FabK with varying concentrations of NADH (1.5-fold dilutions from 350 μM to 9.1 μM) at a fixed concentration of Cro-CoA (325 μM) demonstrating NADH substrate inhibition. Standard Michaelis-Menten fit (dashed blue line) and substrate inhibition line (solid black line with dots) shown for comparison. **(B)** Non-linear regression curve fit of velocity of *Cd*FabK with varying concentrations of enoyl substrate Cro-CoA (1.5-fold dilutions from 4500 μM to 78 μM and 0 μM) at a fixed concentration of NADH (125 μM) demonstrating Cro-CoA substrate inhibition. **(C)** Non-linear regression curve fit of velocity of *Cd*FabK with varying concentrations of alternative enoyl substrate octenoyl-CoA (1.5-fold dilutions from 2500 μM to 43 μM and 0 μM) at a fixed concentration of NADH (125 μM) demonstrating octenoyl-CoA substrate inhibition.

Phenylimidazole-derived compounds selectively inhibit the *C. difficile* FabK enzyme.

Phenylimidazole compounds have been shown to inhibit *Sp*FabK (PDB 2Z6J) and lack inhibitory activity against FabI from *E. coli*.[29, 30] To evaluate activity against *Cd*FabK, phenylimidazole compounds were screened against purified enzyme to determine percent inhibition at 10 μM. Compounds yielding over 50% inhibition were further screened to determine on-target 50% inhibitory concentrations (IC_{50}). Compounds were also screened at 10 μM against purified FabI from *Staphylococcus aureus* (*Sa*FabI) to directly compare activity profiles.

We confirmed the phenylimidazole compounds inhibit *Cd*FabK in a dose-dependent manner. All compounds except **1a**, **1c**, **1d,** and **1h** showed greater than 50% inhibition of *Cd*FabK at 10 μM. IC_{50}s ranged from 7.35 μM with **1g** to 2.86 μM with **1e**, with the series prototype, **1b**, showing an IC_{50} of 3.31 μM. Resulting Hill coefficients from IC_{50} logistic curve fits for **1b**, **1e,** and **1g** were 0.901 (95% Confidence Interval (CI) = 0.761-1.064), 0.8594 (95% CI = 0.6449-1.134), and 1.014 (95% CI = 0.7417-1.365), respectively. These values are not significantly different from unity (Hill slope of 1.000), suggesting these compounds display normal inhibitory behavior and do not bind cooperatively, aggregate, form micelles, or demonstrate problematic insolubility. It also indicates the enzyme's active sites function independently, despite *Cd*FabK being a functional dimer.[27, 28]

All compounds showed IC_{50}s against *Sp*FabK in the sub-micromolar range, with **1b** resulting in an IC_{50} of 67 nM, roughly 49-fold better as compared to *Cd*FabK. Likewise, **1e** and **1g** resulted in respective IC_{50}s of 78 and 85 nM against *Sp*FabK, illustrating roughly 87- and 37-fold better respective IC_{50}s as compared to *Cd*FabK. While activity of **1b** against *Sp*FabK was more potent than against *Cd*FabK, it was still roughly 30 times less potent against *Sp*FabK in our hands than reported elsewhere.[29] As the monomer enzyme concentration used here (50 nM) was lower than that used in previous reports (about 60 nM), the reason for this discrepancy is not readily apparent. FabI was confirmed to be resistant to the phenylimidazole compounds as both **1b** and **AG-205** showed little inhibitory effect against *Sa*FabI with percent inhibition values well below 50% (22.40 and 18.22%, respectively) at 10 μM.

The target specificity profile of *Cd*FabK was examined via activity in the presence of triclosan—a well-known, potent, slow-binding inhibitor of the FabI isozyme.[47] To verify our own methods, triclosan was confirmed to be a potent inhibitor of *Sa*FabI, with nearly 90% inhibition at 10 μM. Like *Sp*FabK, *Cd*FabK proved to be resistant to triclosan at 100 μM and IC_{50} values were not determined.

Phenylimidazole compound 1b is competitive for NADH and uncompetitive for the enoyl substrate against *Cd*FabK

To elucidate the modality of inhibition of the phenylimidazole compounds against *Cd*FabK, we analyzed the inhibitory activity of **1b** against purified enzyme in the presence of varying concentrations of NADH while holding Cro-CoA constant, and likewise in the presence of varying concentrations of Cro-CoA while holding NADH constant. Both non-linear fits and Lineweaver-Burk plots were analyzed. The best non-linear fits for each substrate suggest that **1b** acts as a competitive inhibitor of *Cd*FabK with respect to NADH ($R^2 = 0.91$) and an uncompetitive inhibitor with respect to Cro-CoA ($R^2 = 0.90$). The Lineweaver-Burk plots for each substrate corroborate these findings (**Figure 3**).

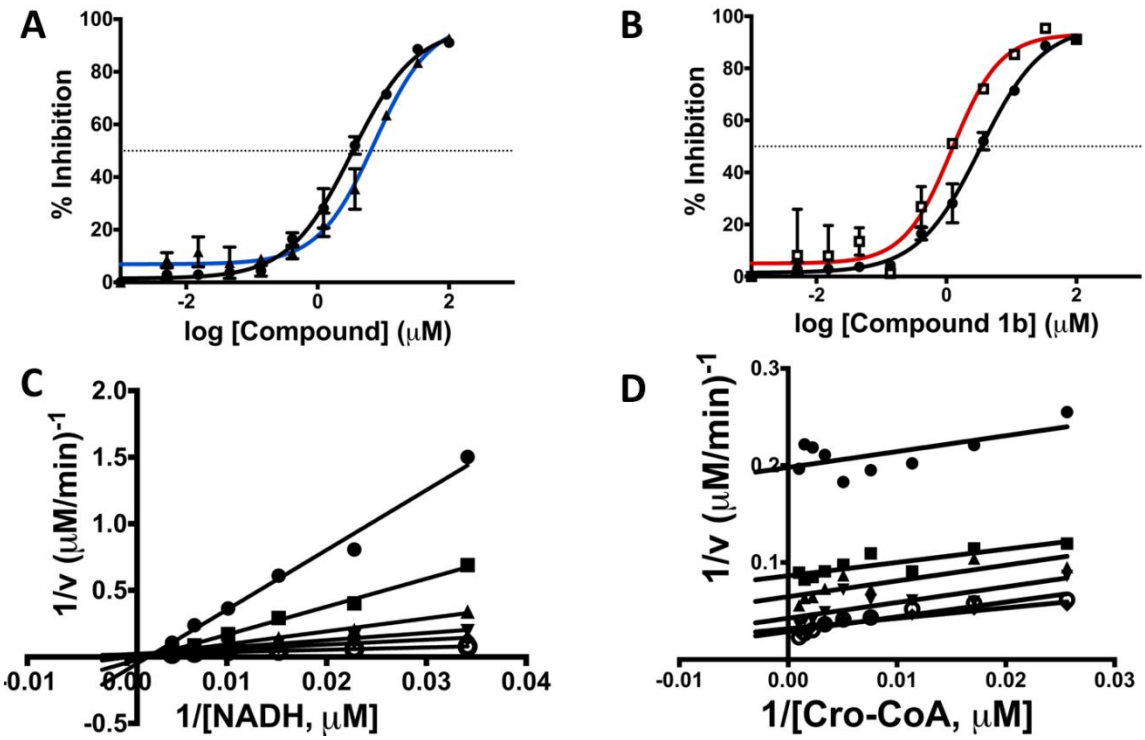

Figure 3. Characterization of Inhibitory Activity and Mechanism of 1b against *Cd*FabK. (A) Sigmoidal plots demonstrating dose response curves for the inhibition of *Cd*FabK by two different phenylimidazole analogues, **1b** (black line with dots) and **1g** (blue line with triangles). **(B)** Sigmoidal plots as dose response curves for the inhibition of *Cd*FabK by **1b** with different concentrations of Cro-CoA, 150 μM Cro-CoA (black line with dots) and 325 μM Cro-CoA (red line with squares). **(C)** Lineweaver-Burk plot showing competitive inhibition of *Cd*FabK binding NADH by **1b**. *Cd*FabK was incubated with varying concentrations of **1b** and NADH at a fixed concentration of Cro-CoA (325 μM). Concentrations of **1b** were 33 μM (closed circle), 11 μM (square), 3.67 μM (triangle), 1.22 μM (upside-down triangle), 0.4 μM (diamond), and 0 μM (open circle). **(D)** Lineweaver-Burk plot showing uncompetitive inhibition of *Cd*FabK binding Cro-CoA by **1b**. *Cd*FabK was incubated with varying concentrations of **1b** and Cro-CoA at a fixed concentration of NADH (150 μM). Concentrations of **1b** were 33 μM (closed circle), 11 μM (square), 3.67 μM (triangle), 1.22 μM (upside-down triangle), 0.4 μM (diamond), and 0 μM (open circle).

Phenylimidazole 1b, 1e, 1f, and 1g selectively inhibited *C. difficile* growth over other key gut flora

Activities of four phenylimidazole derivatives **1b**, **1e**, **1f,** and **1g** were tested against *C. difficile* and representative gut flora (**Table 2**). Tests were done in the presence and absence of the efflux pump inhibitor verapamil, as **1b** was shown to be susceptible to efflux in the strain *C. difficile* CD630.[25] The anti-*C. difficile* MICs of **1b, 1e, 1f,** and **1g** ranged from 4-8 μM and 2-4 μM, in the absence and presence of verapamil. In general, the MICs of the compounds only differed by 2-fold. While vancomycin's anti-*C. difficile* activity (0.4-1.6 μM) was superior, it also inhibited the growth of the representative gut flora, whereas the phenylimidazole compounds did not, even up to 128 μM.

Discussion

We report here the kinetic evaluation of *Cd*FabK, the biochemical activity of a series of phenylimidazole analogues, and microbiological data suggesting these compounds' selective antibacterial activity against *C. difficile* over several other prominent gut organisms. The compounds display promising, low micromolar *Cd*FabK inhibitory activity without significantly affecting the in vitro growth of important gut organisms. *Cd*FabK biochemical activity assays confirmed the inhibitory activity of all phenylimidazole analogues against *Cd*FabK, with several showing potent, low micromolar activity. This data further demonstrates the enzyme's druggability and the potential of the phenylimidazole compounds as leads for developing a novel series of narrow-spectrum anti-*C. difficile* drug candidates. As the imidazole and thiazole-urea moieties in the first-generation inhibitor **1b** were predicted in modeling studies to establish three hydrogen bond interactions, and thus play a significant role in FabK binding, initial structure activity relationship (SAR) and physicochemical exploration during druggability validation was focused on the 4-bromo-phenyl region of the molecule (**Figure 4**, **Scheme 1**). The observed and calculated solubility of **1b** is poor (average solubility 0.36 μM via Biomeck and 0.01 μM via LC/MS). Therefore, in this work, a new expanded set of substituents with different lipophilic and electronic properties was

introduced in the tail region to further probe existing SAR as well as enhance solubility. Specifically, six new compounds **1c-1h**, along with two known compounds **1a-b**, were synthesized (**Scheme 1**) and subsequently evaluated and, while chemical modifications did not substantially increase potency, IC_{50} values indicate inhibitory activity was not abolished despite crucial solubility enhancement via modification at this region. This is illustrated by comparing **1b** (4-bromophenyl, cLogP 4.56 and IC_{50} 3.31 μM) and **1g** (4-cyanophenyl, significantly improved cLogP 3.15, similar IC_{50} 7.35 μM). Because the target enzyme's natural, in vivo function involves the binding of relatively lipophilic fatty acid precursor substrates, this was a noteworthy discovery that will serve as an important structural basis for future inhibitor design and synthesis. While **1e** and **1f** showed MIC values similar in potency to **1b** and **1g**, increased cLogP values (4.6 and 4.8, respectively) for both compounds preclude them from further assessment.

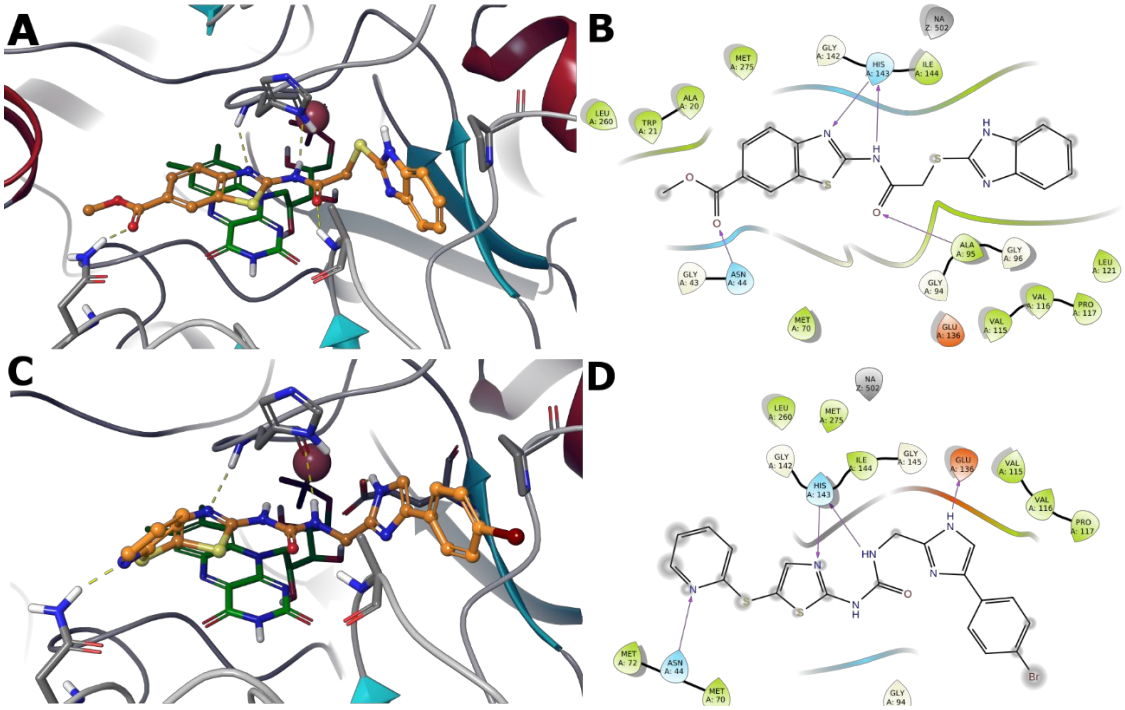

Figure 4. FabK Inhibitors. **A.** AG-205 hit compound shown docked into *Cd*FabK model. Hydrogen bonds indicated by yellow dashes. **B.** 2D ligand interaction diagram of AG-205 bound to *Cd*FabK active site. **C.** phenylimidazole inhibitor **1b** shown docked into *Cd*FabK model. **D.** 2D ligand interaction diagram of **1b** bound to *Cd*FabK active site. See Supporting Information for Materials and Methods.

A high degree of primary sequence identity and active site similarity exists between *Cd*FabK and *Sp*FabK (58% overall identity, 74% overall similarity, and 1% gaps with 2 missing loops on *Sp*FabK, PDB 2Z6J; 100% and 91% active site identity within 3 Å and 4Å from bound inhibitors, respectively, **Figure S1**; residues shown interacting with modeled inhibitors are 100% conserved between *Cd*FabK and *Sp*FabK, **Figure 4**). Despite this, the phenylimidazole compounds showed greater activity against *Sp*FabK than *Cd*FabK (sub-micromolar vs. low micromolar, respectively). The compounds, along with triclosan, were tested against both FabK and FabI to determine comparative FAS-II inhibition profiles. The compounds potently inhibited FabK but lacked activity against FabI, while triclosan potently inhibited FabI but lacked activity against FabK. The reason for the potency disparity of phenylimidazoles against the two similar FabK enzymes is not readily apparent. The mode of inhibition for the phenylimidazoles was reported to be competitive inhibition of *Sp*FabK binding NADH and uncompetitive of *Sp*FabK binding Cro-CoA,[28] and confirmed here to be the same against *Cd*FabK (**Figure 2**) and therefore not the cause for potency dissimilarity. Evaluation at incorrect K_m^{app} values of substrate and cofactor was another potential cause for dissimilar potencies, therefore a substrate inhibition model was considered, increasing the K_m^{app} of Cro-CoA to 327 μM, up from 176 μM seen with a standard Michaelis-Menten model. After re-testing **1b** against *Cd*FabK with 325 μM Cro-CoA, the IC_{50} dropped from 3.31 μM to 1.27 μM. While this resulted in an IC_{50} closer to that observed against *Sp*FabK, it still represents a roughly 19-fold increase and, therefore, also fails to fully explain the discrepancy. A final consideration is the possibility that the unique requirement of *C. difficile* for branched chain fatty acids may impact the substrate requirements of *Cd*FabK, making a branched enoyl substrate more appropriate than Cro-CoA for compound screening, or even introducing the possibility of additional medicinal chemistry modifications to be made to the phenylimidazole compounds suited specifically to *Cd*FabK.

With the continued use of broad-spectrum antibiotics, the increasingly diminishing spectrum of useful anti-CDI antibacterial agents, and the increased incidence of new pathogenic strains, the need for novel antibacterial agents targeting *C. difficile* continues to outpace their discovery. As demonstrated in these studies, a notably attractive target for antibacterial development resides in the bacterial FAS II pathway,

which is structurally dissimilar from the mammalian fatty-acid synthesis (FAS I) pathway.[48] FAS II also contains a number of dissimilar, independent enzymes and enzyme homologues collectively responsible for the synthesis of important bacterial fatty acid precursors and, therefore, appears inherently well-suited for selective targeting.[25, 49] Additionally, the pathway has now been well-validated as being essential in both Gram-negative bacteria and a number of Gram-positive bacteria, even in the presence of exogenous fatty acids. Via direct comparison here of the phenylimidazole compounds' IC_{50} values against different purified enoyl-ACP reductase enzymes from different organisms, the selective druggability of *Cd*FabK can be confirmed. Furthermore, analysis of in vitro MIC values of selected compounds against a panel of key gut microbes in the presence and absence of an efflux pump inhibitor further illustrates this. As such, the selective inhibition of *Cd*FabK represents a particularly promising pathway for future narrow-spectrum anti-difficile development. In vivo efficacy, toxicity, and dysbiosis studies in animal models of phenylimidazoles and derivatives will be indispensable for continued development and, therefore, are anticipated for future studies. Furthermore, as more information pertaining to the human microbiome continues to surface, an ongoing analysis of the distribution of current and novel FAS-II isozymes across the increasing number of known gut microbes will be of critical importance. Such analyses will guide an evolving understanding of the extent of antibacterial specificity and overall promise that targeting FabK truly offers.

Materials and Methods

Chemical synthesis. Compounds **1a-h** were synthesized by following literature procedures with modifications (**Scheme 1**).[25, 29, 30, 50, 51] In brief, amine intermediates **5** were synthesized from benzyl(cyanomethyl)carbamate **2** in 3 steps. Firstly, **2** was treated with sodium methoxide in methanol for 8 h, followed by the addition of ammonium chloride and stirring for 3 days to afford amidine **3** in 91% yield as an HCl salt. Amidine HCl salt **3** was refluxed with a substituted 2-bromoacetophenone and potassium carbonate in THF/water (10:1) for 18 h to afford imidazole derivatives **4**.[30] The Cbz group was removed by refluxing **4** in water and HCl [50] to provide amine intermediates **5**

in 27-69% yields. The carboxamide intermediate **9** was synthesized in two steps from commercially available starting materials. Firstly, 2-mercaptopyridine **6** and 2-amino-5-bromothiazole monohydrobromide **7** were stirred with K_2CO_3 in DMF at 80ºC for 1.5 h under nitrogen atmosphere to afford **8** in 67% yield after flash column chromatography. Compound **8** was reacted with 1,1'-carbonyldiimidazole (CDI) [51] in DCM to afford intermediate **9** in 74% yield after filtration and washing solid with DCM. Finally, compounds **1a-g** were obtained by reacting **9** with substituted amine **5** in chloroform and triethylamine for 1 h. The reactions were filtered, diluted with $CHCl_3$ (50 mL), washed with water (50 mL × 3), and concentrated to give **1a-g** in pure form and 30-89% yields after trituration with DCM/diethyl ether (1:1) (**Scheme 1**). Compound **1h** was obtained in excellent yield via the demethylation of **1d** using BBr_3 in DCM. Complete general chemistry and procedures, reagents and conditions, characterization data with ^1H and ^{13}C NMR spectra, as well as HPLC chromatograms for phenylimidazole compounds can be found in the Supporting Information.

Enzyme expression and purification. The *Cd*FabK and *Sp*FabK enzymes were expressed and purified to homogeneity and confirmed as reported elsewhere.[25] *Sa*FabI was produced in high yield and purity as reported elsewhere in the literature.[52] *Sa*FabI was confirmed via PAGE gel analysis and enzyme activity assay analysis in an Implen NP80 nanophotometer as described below (West Lake Village, CA).

FAS-II biochemical enzyme assays. All compounds were dissolved in DMSO at concentrations of 10 mM, then further diluted in pure DMSO to the required concentrations. Both *Cd*FabK and *Sp*FabK assays were conducted via the following protocol: Reactions were carried out at 25°C in FabK Assay Buffer (100 mM HEPES pH 8.0, 500 mM NH_4Cl, 10% glycerol, and 0.125 mg/mL γ-Globulins; 10% DMSO) with 150 μM Cro-CoA and 150 μM NADH. Compounds were incubated in three-fold dilutions (ranging from 100 μM to 5 nM for *Cd*FabK and 33 μM to 1.7 nM for *Sp*FabK) in the presence of 50 nM target enzyme. Compounds and enzyme were incubated together for 10 minutes before the Cro-CoA substrate was added and the reaction was started immediately afterward via the addition of NADH. NADH fluorescence (340

nm/460 nm) was measured in a Biotek Synergy H1 microplate reader (Winooski, VT) in a final volume of 100 μL in Greiner Bio-One™ 384-Well μClear™ Bottom Polystyrene Microplates (Monroe, NC) via 20 second intervals for 10 minutes to evaluate the rate of reaction.

*Sa*FabI assays were conducted at 25° C in FabI Assay Buffer (50 mM MES pH 5.5, 150 mM NaCl, 10 mM EDTA, and 2% DMSO) with 300 μM NADPH and 1 mM Cro-CoA. Compounds were incubated at 10 μM with 500 nM *Sa*FabI for 20 minutes. Reactions were started via the addition of NADPH. NADPH absorbance was measured (340 nm) every 10 seconds for 10 minutes in a final volume of 100 μL to evaluate the rate of reaction.

FabK IC_{50} calculations and kinetics. Starting at three minutes, linear slopes were measured for three additional minutes and used to determine the reaction rates. Measurements were conducted in duplicate and IC_{50}s were calculated via GraphPad Prism 7.0d (La Jolla, CA) using four-parameter logistic (Hill) curve analysis using the equation Y = Bottom + (Top – Bottom)/[1+10^((LogIC50 – X)*HillSlope)], where X is logarithm of dose and Y is response. Kinetics with respect to cofactor and substrates were also assessed via GraphPad Prism 7.0d comparing both Michaelis-Menten and substrate inhibition models.

FabI activity. Starting at two minutes, linear slopes were measured for three minutes and used to determine the reaction rates. Measurements were conducted in duplicate and percent inhibitions were calculated against un-inhibited enzyme.

MICs in select gut flora. The strains used in this study are listed in **Table 2**. The susceptibility tests to various compounds were performed in microtiter 96-well plate as described previously.[25] The MIC tests were performed in BHI broth for *C. difficile*, *C. perfringens* and *B. ovatus*, whereas Bifidobacterium broth (Himedia) was used for *B. breve* strains. These strains were grown at 37ºC in a Don Whitley A35 anaerobic chamber. Susceptibility testing against *S. pyogenes* was performed in aerobic growth

conditions in BHI-TY and Muller Hinton broth, respectively. Susceptibility tests were performed in presence or absence of the efflux pump inhibitor verapamil (50 μg/ml). MICs are reported as the lowest concentration of compound that inhibited bacterial growth of respective test organisms.

Acknowledgements

We thank Y. Li, X. Fu, and L. Yang at St. Jude Children's Research Hospital for ADME studies on compound **1b**. Table of Contents figure created with BioRender. Molecular graphics and analyses (Figure 1) performed with UCSF Chimera, developed by the Resource for Biocomputing, Visualization, and Informatics at the University of California, San Francisco, with support from NIH P41-GM103311.

Funding Sources

We are grateful to the National Institute of Allergy and Infectious Diseases of the National Institutes of Health for funding (R21AI126755). This research was also made possible by the American Foundation for Pharmaceutical Education, Pre-Doctoral Award in Pharmaceutical Sciences to JAJ and by the Center for Pediatric Experimental Therapeutics (CPET) via financial support to JAJ as a CPET scholar.

Supporting Information

Supporting information, including a sequence alignment comparing *Cd*FabK to *Sp*FabK; as well as the methods pertaining to the sequence alignment, general chemistry synthesis and procedure for phenylimidazole compounds, spectral analysis of phenylimidazole compounds and HPLC purity, homology modeling of *C. difficile* FabK, and molecular docking and modeling of *C. difficile* FabK inhibitors, is available online: This material is available free of charge via the internet at http://pubs.acs.org.

References

1. Gil, F., Calderon, I. L., Fuentes, J. A., and Paredes-Sabja, D. (2018) Clostridioides (Clostridium) difficile infection: current and alternative therapeutic strategies, *Future Microbiol. 13*, 469-482.

2. Dubberke, E. R., and Olsen, M. A. (2012) Burden of Clostridium difficile on the healthcare system, *Clin. Infect. Dis. 55 Suppl 2*, S88-92.

3. Lessa, F. C., Gould, C. V., and McDonald, L. C. (2012) Current status of Clostridium difficile infection epidemiology, *Clin. Infect. Dis. 55 Suppl 2*, S65-70.

4. Antharam, V. C., Li, E. C., Ishmael, A., Sharma, A., Mai, V., Rand, K. H., and Wang, G. P. (2013) Intestinal dysbiosis and depletion of butyrogenic bacteria in Clostridium difficile infection and nosocomial diarrhea, *J. Clin. Microbiol. 51*, 2884-2892.

5. Crawford, T., Huesgen, E., and Danziger, L. (2012) Fidaxomicin: a novel macrocyclic antibiotic for the treatment of Clostridium difficile infection, *Am. J. Health Syst. Pharm. 69*, 933-943.

6. Tsutsumi, L. S., Owusu, Y. B., Hurdle, J. G., and Sun, D. (2014) Progress in the discovery of treatments for *C. difficile* infection: A clinical and medicinal chemistry review, *Curr. Top. Med. Chem. 14*, 152-175.

7. Marsh, J. W., Arora, R., Schlackman, J. L., Shutt, K. A., Curry, S. R., and Harrison, L. H. (2012) Association of relapse of Clostridium difficile disease with BI/NAP1/027, *J. Clin. Microbiol. 50*, 4078-4082.

8. Garey, K. W., Sethi, S., Yadav, Y., and DuPont, H. L. (2008) Meta-analysis to assess risk factors for recurrent Clostridium difficile infection, *J. Hosp. Infect. 70*, 298-304.

9. Lewis, B. B., Carter, R. A., Ling, L., Leiner, I., Taur, Y., Kamboj, M., Dubberke, E. R., Xavier, J., and Pamer, E. G. (2017) Pathogenicity Locus, Core Genome, and Accessory Gene Contributions to Clostridium difficile Virulence, *MBio 8*.

10. Francino, M. P. (2015) Antibiotics and the Human Gut Microbiome: Dysbioses and Accumulation of Resistances, *Front. Microbiol. 6*, 1543.

11. Louie, T. J., Miller, M. A., Mullane, K. M., Weiss, K., Lentnek, A., Golan, Y., Gorbach, S., Sears, P., Shue, Y. K., and Group, O. P. T. C. S. (2011) Fidaxomicin versus vancomycin for Clostridium difficile infection, *N. Engl. J. Med. 364*, 422-431.

12. Orenstein, R. (2012) Fidaxomicin failures in recurrent Clostridium difficile infection: a problem of timing, *Clin. Infect. Dis. 55*, 613-614.

13. Angelakis, E., Armougom, F., Million, M., and Raoult, D. (2012) The relationship between gut microbiota and weight gain in humans, *Future Microbiol. 7*, 91-109.

14. McDonald, L. C., Gerding, D. N., Johnson, S., Bakken, J. S., Carroll, K. C., Coffin, S. E., Dubberke, E. R., Garey, K. W., Gould, C. V., Kelly, C., Loo, V., Shaklee Sammons, J., Sandora, T. J., and Wilcox, M. H. (2018) Clinical Practice Guidelines for Clostridium difficile Infection in Adults and Children: 2017 Update by the Infectious Diseases Society of America (IDSA) and Society for Healthcare Epidemiology of America (SHEA), *Clin. Infect. Dis. 66*, e1-e48.

15. Petrosillo, N., Granata, G., and Cataldo, M. A. (2018) Novel Antimicrobials for the Treatment of Clostridium difficile Infection, *Front. Med. (Lausanne) 5*, 96.

16. Pedrido, M. E., de Ona, P., Ramirez, W., Lenini, C., Goni, A., and Grau, R. (2013) Spo0A links de novo fatty acid synthesis to sporulation and biofilm development in Bacillus subtilis, *Mol. Microbiol. 87*, 348-367.

17. Heath, R. J., and Rock, C. O. (2004) Fatty acid biosynthesis as a target for novel antibacterials, *Curr. Opin. Investig. Drugs 5*, 146-153.

18. Karlowsky, J. A., Kaplan, N., Hafkin, B., Hoban, D. J., and Zhanel, G. G. (2009) AFN-1252, a FabI inhibitor, demonstrates a Staphylococcus-specific spectrum of activity, *Antimicrob. Agents Chemother. 53*, 3544-3548.

19. Parsons, J. B., Kukula, M., Jackson, P., Pulse, M., Simecka, J. W., Valtierra, D., Weiss, W. J., Kaplan, N., and Rock, C. O. (2013) Perturbation of Staphylococcus aureus gene expression by the enoyl-acyl carrier protein reductase inhibitor AFN-1252, *Antimicrob. Agents Chemother. 57*, 2182-2190.

20. Hunt, T., Kaplan, N., and Hafkin, B. (2016) Safety, tolerability and pharmacokinetics of multiple oral doses of AFN-1252 administered as immediate release (IR) tablets in healthy subjects, *J. Chemother. 28*, 164-171.

21. Heath, R. J., Su, N., Murphy, C. K., and Rock, C. O. (2000) The enoyl-[acyl-carrier-protein] reductases FabI and FabL from Bacillus subtilis, *J. Biol. Chem. 275*, 40128-40133.

22. Marrakchi, H., Dewolf, W. E., Jr., Quinn, C., West, J., Polizzi, B. J., So, C. Y., Holmes, D. J., Reed, S. L., Heath, R. J., Payne, D. J., Rock, C. O., and Wallis, N. G. (2003) Characterization of Streptococcus pneumoniae enoyl-(acyl-carrier protein) reductase (FabK), *Biochem. J. 370*, 1055-1062.

23. Massengo-Tiasse, R. P., and Cronan, J. E. (2008) Vibrio cholerae FabV defines a new class of enoyl-acyl carrier protein reductase, *J. Biol. Chem. 283*, 1308-1316.

24. Stabler, R. A., He, M., Dawson, L., Martin, M., Valiente, E., Corton, C., Lawley, T. D., Sebaihia, M., Quail, M. A., Rose, G., Gerding, D. N., Gibert, M., Popoff, M. R., Parkhill, J., Dougan, G., and Wren, B. W. (2009) Comparative genome and phenotypic analysis of Clostridium difficile 027 strains provides insight into the evolution of a hypervirulent bacterium, *Genome Biol. 10*, R102.

25. Marreddy, R. K. R., Wu, X., Sapkota, M., Prior, A. M., Jones, J. A., Sun, D., Hevener, K. E., and Hurdle, J. G. (2019) The Fatty Acid Synthesis Protein Enoyl-ACP Reductase II (FabK) is a Target for Narrow-Spectrum Antibacterials for Clostridium difficile Infection, *ACS Infect. Dis. 5*, 208-217.

26. Heath, R. J., and Rock, C. O. (2000) A triclosan-resistant bacterial enzyme, *Nature 406*, 145-146.

27. Hevener, K. E., Santarsiero, B. D., Lee, H., Jones, J. A., Boci, T., Johnson, M. E., and Mehboob, S. (2018) Structural characterization of Porphyromonas gingivalis enoyl-ACP reductase II (FabK), *Acta Crystallogr. F Struct. Biol. Commun. 74*, 105-112.

28. Saito, J., Yamada, M., Watanabe, T., Iida, M., Kitagawa, H., Takahata, S., Ozawa, T., Takeuchi, Y., and Ohsawa, F. (2008) Crystal structure of enoyl-acyl carrier protein reductase (FabK) from Streptococcus pneumoniae reveals the binding mode of an inhibitor, *Protein Sci. 17*, 691-699.

29. Ozawa, T., Kitagawa, H., Yamamoto, Y., Takahata, S., Iida, M., Osaki, Y., and Yamada, K. (2007) Phenylimidazole derivatives as specific inhibitors of bacterial enoyl-acyl carrier protein reductase FabK, *Biorg. Med. Chem. 15*, 7325-7336.

30. Kitagawa, H., Ozawa, T., Takahata, S., Iida, M., Saito, J., and Yamada, M. (2007) Phenylimidazole derivatives of 4-pyridone as dual inhibitors of bacterial enoyl-acyl carrier protein reductases FabI and FabK, *J. Med. Chem. 50*, 4710-4720.

31. Kitagawa, H., Ozawa, T., Takahata, S., and Iida, M. (2007) Phenylimidazole derivatives as new inhibitors of bacterial enoyl-ACP reductase FabK, *Bioorg. Med. Chem. Lett. 17*, 4982-4986.

32. Takahata, S., Iida, M., Osaki, Y., Saito, J., Kitagawa, H., Ozawa, T., Yoshida, T., and Hoshiko, S. (2006) AG205, a novel agent directed against FabK of Streptococcus pneumoniae, *Antimicrob. Agents Chemother. 50*, 2869-2871.

33. Saito, J., Yamada, M., Watanabe, T., Kitagawa, H., and Takeuchi, Y. (2006) Crystallization and preliminary X-ray analysis of enoyl-acyl carrier protein reductase (FabK) from Streptococcus pneumoniae, *Acta Crystallogr. Sect. F Struct. Biol. Cryst. Commun. 62*, 576-578.

34. White, S. W., Zheng, J., Zhang, Y. M., and Rock. (2005) The structural biology of type II fatty acid biosynthesis, *Annu. Rev. Biochem. 74*, 791-831.

35. Oppermann, U., Filling, C., Hult, M., Shafqat, N., Wu, X., Lindh, M., Shafqat, J., Nordling, E., Kallberg, Y., Persson, B., and Jornvall, H. (2003) Short-chain dehydrogenases/reductases (SDR): the 2002 update, *Chem. Biol. Interact. 143-144*, 247-253.

36. Brinster, S., Lamberet, G., Staels, B., Trieu-Cuot, P., Gruss, A., and Poyart, C. (2009) Type II fatty acid synthesis is not a suitable antibiotic target for Gram-positive pathogens, *Nature 458*, 83-86.

37. Balemans, W., Lounis, N., Gilissen, R., Guillemont, J., Simmen, K., Andries, K., and Koul, A. (2010) Essentiality of FASII pathway for Staphylococcus aureus, *Nature 463*, E3; discussion E4.

38. Brinster, S., Lamberet, G., Staels, B., Trieu-Cuot, P., Gruss, A., and Poyart, C. (2010) Brinster, Lamberet, Staels, Trieu-Cuot, Gruss, & Poyart, reply, *Nature 463*, E4-E5.

39. Parsons, J. B., and Rock, C. O. (2011) Is bacterial fatty acid synthesis a valid target for antibacterial drug discovery?, *Curr. Opin. Microbiol. 14*, 544-549.

40. Parsons, J. B., and Rock, C. O. (2013) Bacterial lipids: metabolism and membrane homeostasis, *Prog. Lipid Res. 52*, 249-276.

41. Goldfine, H., and Johnston, N. C. (2004) Membrane Lipids of Clostridia, In *Handbook on Clostridia* (Duerre, P., Ed.), pp 297-309, CRC Press.

42. Guan, Z., Katzianer, D., Zhu, J., and Goldfine, H. (2014) Clostridium difficile contains plasmalogen species of phospholipids and glycolipids, *Biochim. Biophys. Acta 1842*, 1353-1359.

43. Pettersen, E. F., Goddard, T. D., Huang, C. C., Couch, G. S., Greenblatt, D. M., Meng, E. C., and Ferrin, T. E. (2004) UCSF Chimera--a visualization system for exploratory research and analysis, *J. Comput. Chem. 25*, 1605-1612.

44. Arumugam, M., Raes, J., Pelletier, E., Le Paslier, D., Yamada, T., Mende, D. R., Fernandes, G. R., Tap, J., Bruls, T., Batto, J. M., Bertalan, M., Borruel, N., Casellas, F., Fernandez, L., Gautier, L., Hansen, T., Hattori, M., Hayashi, T., Kleerebezem, M., Kurokawa, K., Leclerc, M., Levenez, F., Manichanh, C., Nielsen, H. B., Nielsen, T., Pons, N., Poulain, J., Qin, J., Sicheritz-Ponten, T., Tims, S., Torrents, D., Ugarte, E., Zoetendal, E. G., Wang, J., Guarner, F., Pedersen, O., de Vos, W. M., Brunak, S., Dore, J., Meta, H. I. T. C., Antolin, M., Artiguenave, F., Blottiere, H. M., Almeida, M., Brechot, C., Cara, C., Chervaux, C., Cultrone, A., Delorme, C., Denariaz, G., Dervyn, R., Foerstner, K. U., Friss, C., van de Guchte, M., Guedon, E., Haimet, F., Huber, W., van Hylckama-Vlieg, J., Jamet, A., Juste, C., Kaci, G., Knol, J., Lakhdari, O., Layec, S., Le Roux, K., Maguin, E., Merieux, A., Melo Minardi, R., M'Rini, C., Muller, J., Oozeer, R., Parkhill, J., Renault, P., Rescigno, M., Sanchez, N., Sunagawa, S., Torrejon, A., Turner, K., Vandemeulebrouck, G., Varela, E., Winogradsky, Y., Zeller, G., Weissenbach, J., Ehrlich, S. D., and Bork, P. (2011) Enterotypes of the human gut microbiome, *Nature 473*, 174-180.

45. Zheng, C. J., Sohn, M. J., Lee, S., and Kim, W. G. (2013) Meleagrin, a new FabI inhibitor from Penicillium chryosogenum with at least one additional mode of action, *PLoS One 8*, e78922.

46. Yao, J., Ericson, M. E., Frank, M. W., and Rock, C. O. (2016) Enoyl-Acyl Carrier Protein Reductase I (FabI) Is Essential for the Intracellular Growth of Listeria monocytogenes, *Infect. Immun. 84*, 3597-3607.

47. Priyadarshi, A., Kim, E. E., and Hwang, K. Y. (2010) Structural insights into Staphylococcus aureus enoyl-ACP reductase (FabI), in complex with NADP and triclosan, *Proteins 78*, 480-486.

48. Kingry, L. C., Cummings, J. E., Brookman, K. W., Bommineni, G. R., Tonge, P. J., and Slayden, R. A. (2013) The Francisella tularensis FabI enoyl-acyl carrier protein reductase gene is essential to bacterial viability and is expressed during infection, *J. Bacteriol. 195*, 351-358.

49. Khan, R., Zeb, A., Roy, N., Thapa Magar, R., Kim, H. J., Lee, K. W., and Lee, S. W. (2018) Biochemical and Structural Basis of Triclosan Resistance in a Novel Enoyl-Acyl Carrier Protein Reductase, *Antimicrob. Agents Chemother. 62*, pii: e00648-00618.

50. Chelucci, G., Falorni, M., and Giacomelli, G. (1990) Synthesis of 1-Substituted 2-[(2s)-2-Pyrrolidinyl]Pyridine from L-Proline, *Synthesis-Stuttgart 1990*, 1121-1122.

51. Rawling, T., McDonagh, A. M., Tattam, B., and Murray, M. (2012) Synthesis of unsymmetrical biaryl ureas from N-carbamoylimidazoles: kinetics and application, *Tetrahedron 68*, 6065-6070.

52. Schiebel, J., Chang, A., Lu, H., Baxter, M. V., Tonge, P. J., and Kisker, C. (2012) Staphylococcus aureus FabI: inhibition, substrate recognition, and potential implications for in vivo essentiality, *Structure 20*, 802-813.

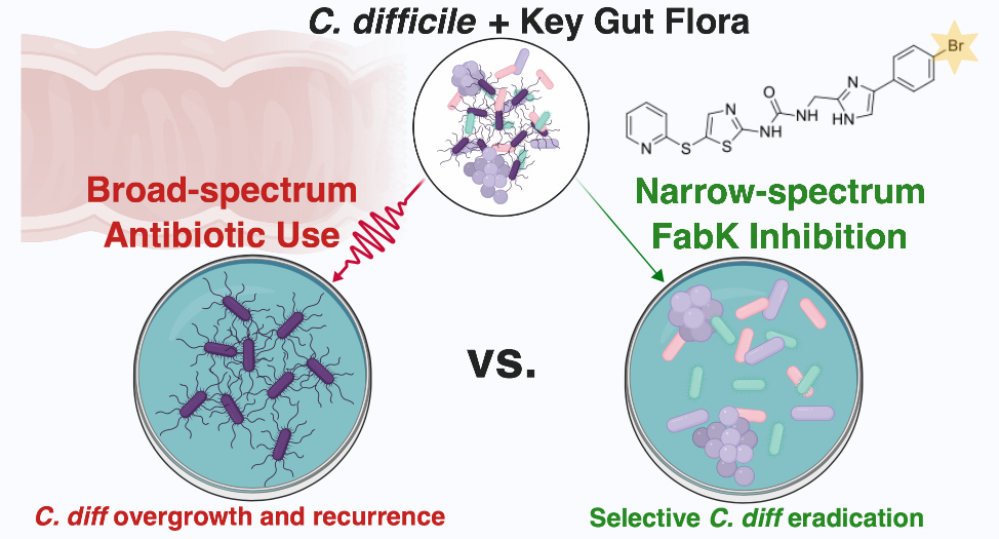

82x44mm (300 x 300 DPI)